Accepted for presentation in: 3rd International Conference on 6G Networking (6GNet), Paris, France, October 2024.

Design Aspects for Efficient Beam Training in 6G Millimeter-Wave Networks with Mobile Users

Simon Häger*, Bara Sabbah*, and Christian Wietfeld*

***Abstract*—With 6G millimeter-wave (mmWave) networks aiming to make their services available to mobile users, beam management procedures need to be reevaluated. Many studies have focused on link maintenance for mobile users already connected to the network, however, little is known about the implications of mobile users intending to access the network. Beam training design trade-offs in terms of data rate, delay, and coverage area have been observed in studies with stationary users. This work builds on this state-of-the-art by investigating the differences between stationary and mobile initial access along these metrics. We find that the exhaustive search algorithm's optimal performance degrades rapidly for mobile users by selecting stale beam pairs, for example, resulting in tens of decibel power loss and, particularly, failure in more than 80 % of the initial access at 45 km/h owing to the high search duration. This problem can be shifted to higher velocities by using broader beams for lower delay, but at the cost of decreased coverage. Instead, our work highlights that beam training for mobile users should terminate immediately once a beam pair of a desirable quality is found to avoid staleness. By lowering the target threshold of our proposed scheme, the delay is minimized at the cost of selecting less-robust links. However, we demonstrate that there is a sweet spot that minimizes delay while maximizing the link strength, and thereby also enabling users at typical urban velocities to access the network at a negligible failure risk by minimizing loss.**

I. Introduction

Increasing cellular traffic has sparked the extension to mmWave frequencies, as the available broad bands allow for a scalable increase in network capacity and peak data rates. There, however, deteriorated propagation characteristics reduce the cell sizes. Beamforming antenna arrays are employed by base station (BS) and user equipment (UE) for compensation, but their beam orientations need to be well-aligned by novel beam management procedures for ample gain [1].

Numerous works address the link maintenance for mobile mmWave users, e.g., by beam tracking which requires frequent updates of the beams' orientations and widths along the trajectory [2, 3]. What is more complex is the realization of beam switching once the current propagation path becomes infeasible, e.g., by moving into a building shadow. In this case, it is required to switch to a non-line-of-sight (NLOS) path or to another cell [4]. Yet, the above considerations refer to mobile users that have already successfully registered in the network. Prior to this, there is the challenge of link establishment as both UE and BS have to find suitable beam orientations in azimuth and elevation planes. This may significantly prolong the cell search procedure [5]. Most research works consider different beam training algorithms under stationary conditions [6], but if the user moves during the beam training, stale data might lead to the establishment of poor links, i.e., with reduced data rate and lower robustness to the ongoing user mobility, or worse, even initial access failures (IAFs), see Fig. 1. Hence, this could disrupt the market success of future 6G mmWave networks such that mobility aspects must be analyzed to develop optimized beam training algorithms [7].

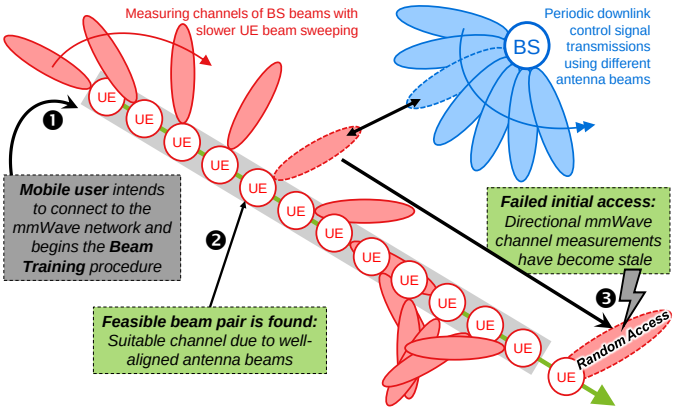

Fig. 1. 5G mmWave networks mainly facilitate stationary users, but 6G aims to reliably support mobile users as well [7]. However, lengthy beam training procedures for directional link establishment can be disrupted by mobility-induced stale channel data. This work thus examines the effects of mobility and explores design strategies for efficient mobile initial access.

Against this background, we contribute the following aspects to the ongoing research on 6G mmWave communications:

- First in-depth assessment of the impact of user mobility during and after beam training compared to stationary mmWave initial access conditions.
- Comprehensive ray-tracing-based performance evaluation incorporates existing design trade-offs for beam training schemes in an urban outdoor scenario.
- Proposal of design recommendations for beam training supporting mobile users directly applied to a novel parametrizable beam search algorithm.

The remainder of this work is structured as follows. In Sec. II we discuss related work on beam training which is followed up with a brief experimental case study on mobile beam training in Sec. III. Afterward, Sec. IV describes the methodology of this work. We then evaluate the impact of the choice of beam training algorithm and antenna beam type on the robustness against user mobility in Sec. V. Last, Sec. VI summarizes the results of this manuscript and gives an outlook on future work.

*The authors are with the Communication Networks Institute (CNI) at TU Dortmund University, Dortmund, Germany. E-mail: {Simon.Haeger, Bara.Sabbah, Christian.Wietfeld}@tu-dortmund.de. Their work has been funded by the German Federal Ministry of Education and Research (BMBF) in the course of the *6GEM Research Hub* under the grant number 16KISK038.

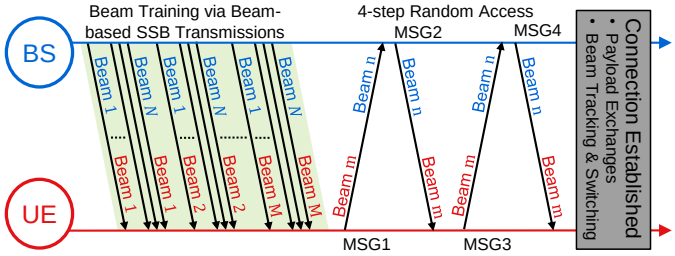

Fig. 2. Initial access using the *exhaustive search* beam training algorithm. At the cost of an excessive delay from $M \cdot N$ measurements, the optimal beam pair (m, n) is identified under stationary conditions.

II. Related Works on mmWave Beam Training

Using antenna beambooks, i.e., a set of predefined beam orientations, the directional channel is attained, at worst, by testing every possible UE and BS beam combination during the 5G initial access procedure, as illustrated in Fig. 2. The BS transmits up to 64 synchronization signal (SS) blocks along different beams within the scope of a 5 ms long SS burst at a high periodicity. In the meantime, the UE also sweeps its beams and tries to identify the best possible BS-UE beam pair for communications. With the selected BS beam also comes the information which time-frequency resources ought to be used to initiate random access to the network. After successful initial access, UE and BS may exchange payload data. Moreover, beam tracking and switching procedures are launched and continued based on regular control signaling [1, 5, 8].

In literature, a wide variety of beam training algorithms aiming to optimize performance have been proposed with the implementation decision being up to equipment vendors [5]: Similar to exhaustive search, there are hierarchical beam search algorithms [9] that, in a first stage, use broad beams to reduce the delay. However, this reduces the cell size for initial access and the likelihood of beam misalignments, and therefore, lower link strength, increases. In contrast, the fast neighbor discovery (FastND) [10] algorithm does not aim to select the optimal beam pair but terminates once a decodable link is found. This does neither guarantee a fixed low delay nor a sufficient link quality for high data rates and robustness against mobility. However, the coverage for initial access is not reduced. Like FastND, various schemes do not have a fixed search order but may alter it based on the measurements, e.g., using compressive sensing techniques, to optimize the performance. This comes at the cost of detailed antenna pattern information, expensive beamforming architectures, and increased computing load [11, 12]. In [13] it is recommend that BS beambooks need to be minimized according to the deployment scenario for additional performance gains. Similarly, radio access technology (RAT)-external context information

Fig. 3. The choice of beam training algorithm and associated beam types results in a three-way trade-off which may need to be extended.

such as mutual position information may also be used but its use is restricted to line-of-sight (LOS) modality, such that regular beam training algorithms are still needed [1]. As such, the latter schemes nonetheless adhere to the initially described three-way beam training design trade-off, as depicted in Fig. 3.

In the context of beam tracking and switching, post-beam training mobility is investigated in several works. It is found in [14] that, without compensation, the link quality deteriorates quickly and even radio link failures (RLFs) may be incurred. Thus, the mobility-induced staleness of measurement data illustrated in Fig. 1 was confirmed, however, potential beam training algorithm-based dependencies were not considered. Moreover, results in [2] indicate that beam search space reductions can be unsuitable for managing mobile mmWave UEs. Few works truly consider mobile beam training with exceptions being [6, 15] in which multi-lobe beams are proposed to reduce search time. This comes at the cost of reduced coverage, cf. Fig. 3, but also at increased beamforming transceiver costs. A further recommendation in [16] is to add dedicated training signaling on the BS side at a higher rate to facilitate beam training for mobile users quicker. This comes with undesired always-on overhead in scenarios where there are only occasionally highly mobile UEs. Owing to this gap in research, we deem it necessary to study mobile beam training.

III. Laboratory Mobile Beam Training Study

This section serves to underline the impact of mobility-induced mmWave channel staleness, as sketched in Fig. 1, with laboratory measurement data. In Sec. III-A, we present the measurement setup before discussing the results in Sec. III-B.

A. Measurement Setup and Methodology of Case Study

In this case study our goal is to investigate mobility-induced distortions when the user moves from position A to B during beam training, as depicted in Fig. 4. We compare the observed channel conditions in angular space to the ones that would have been observed if the UE would have remained stationary. For this purpose, we use our experimental 6G mmWave platform setup which was used recently to validate context-aware beam switching using reflectors [17]. Details on the channel sounding mode are provided in [18]. The channel measurements are conducted for 12,769 BS beam orientations in azimuth (ϕ) and elevation (θ) space combined with 201 UE positions along the rail, cf. Tab. I. The beam sweep begins at start position A with $\phi, \theta = -56°$ and operates in an azimuth-first fashion. Every 1 cm of UE rail movement, 64 BS beam alignments are measured. Eventually, the exhaustive search is completed by the time the UE arrives at the end position B.

B. Comparing Mobile and Stationary mmWave Initial Access

The arising received signal strength (RSS) heatmaps are depicted in Fig. 5. One can see, that the mobile UE's perspective on its environment (cf. Fig. 5c) differs from the real channel conditions at end position B (cf. Fig. 5b): One can easily identify a distinct blur that does not seem too drastic. However, if the UE would initiate the initial access using the random access resources of the BS beam with $(\phi, \theta) = (-6°, 0°)$ it has previously identified to provide the strongest signal, this beam

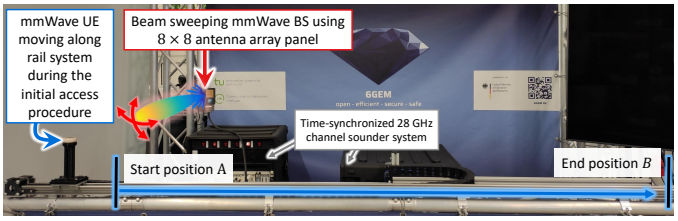

Fig. 4. Mobile beam training scenario during which the UE moves from position A to B and measures the BS's directional downlink SS blocks.

TABLE I. MMWAVE CHANNEL MEASUREMENT SETUP [17, 18].

Parameter	Description/Value
Carrier Frequency	28 GHz (5G band n257) using 1.5 GHz bandwidth
Transmit Power	25 dBm (ca. 300 mW)
BS Antenna	8×8 uniform planar phased array
Beam Sweeping	$\phi, \theta \in [-56°, 56°]$ with 1° resolution
Emulated Signaling	5 ms SS burst periodicity containing 64 SS blocks
UE Antenna	omni-directional antenna
Rail Trajectory	2.0 m from position A to B with 1 cm resolution
Start Position A	LOS distance: 1.37 m, BS angles: $\phi = 34°$, $\theta = 0°$
End Position B	LOS distance: 2.42 m, BS angles: $\phi = -24°$, $\theta = 0°$
Emulated Velocity	2 m/s, i.e., 1 cm per SS burst

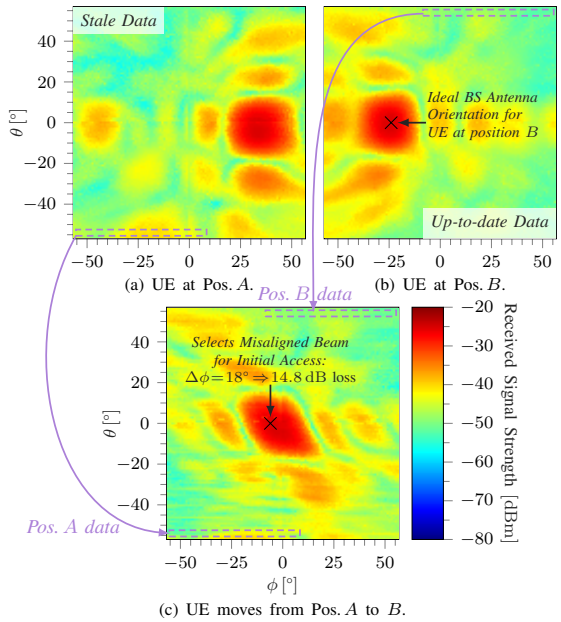

(a) UE at Pos. A. (b) UE at Pos. B.

(c) UE moves from Pos. A to B.

Fig. 5. Beam training-based beam space channel state situation heatmaps: (a)-(b) Stationary case as in literature, (c) mobility-induced distortions.

would not be the ideal choice at position B. To be precise, the selected beam would have an azimuth misalignment of 18° exceeding the pencil beamwidth, and thus, it leads to power loss of 14.8 dB. This will reduce the attained mmWave link's data rate until further beam management procedures correct the beam alignment. As such, we have briefly verified our claims from Secs. I and II that user mobility can have severe impact on the mmWave access. Owing to this, this work now investigates user mobility during and after beam training in more detail by using a large-scale outdoor ray-tracing dataset.

IV. Methodology for mmWave Beam Training Assessment with Urban Ray-Tracing Dataset

This section introduces the methodology of this work with Sec. IV-A first introducing the ray-tracing dataset. Considered types of mobility during and after beam training are discussed in Sec. IV-B. A novel parametrizable beam search algorithm is introduced in Sec. IV-C, which, in combination with different beam types, is used to emulate existing and future beam training protocols' behavior in the well-defined stationary performance metric triangle from Sec. II, cf. Fig. 3. Last, Sec. IV-D recapitulates the performance metrics of this work.

A. Dataset of an Urban Deployment Scenario

This work leverages a 26.5 GHz urban mmWave network dataset, as introduced in detail in [19]. The scenario consists of 20 m-wide urban canyons between 100×100 m-sized buildings, see Fig. 6. Here we consider two BSs mounted 10 m above street level with a fixed equivalent isotropically radiated power (EIRP) of 40 dBm. There are 110,000 UE positions in a 20 cm grid at the height of 1.5 m within our 120×120 m evaluation area. Similar to [18], the decoding threshold on the UE side is at −83.5 dBm for 100 MHz-wide component carriers. The simulations with *Altair WinProp* result in ray information per channel impulse response (CIR) tab: RSS, UE and BS side azimuth (ϕ) and elevation (θ) angles. Based thereon, directional antenna characteristics are imposed by post-processing using *MathWorks MATLAB antenna toolbox*. Either pencil (8×8 phased array (cf. Sec. III), 19.7 dBi gain) or sector beams (4×4, 13.5 dBi) are employed on either side along with respective beambooks, as illustrated in Fig. 7.

Considering the half-power beamwidths (HPBWs) of 12.8° and 26.3° of the pencil and sector beams, cf. Fig. 7, we use either 12° or 24° spacings between the beambook entries to limit beam misalignment-based loss. On BS side, we use the following θ_{BS}: $\{0°, -12°, \ldots, -84°\}$ (8 angles) or $\{0°, -24°, \ldots, -72°\}$ (4 angles) for pencil and sector beams, respectively. The same angles but with a flipped sign are used on the UE side to realize uptilt beam orientations θ_{UE}. Moving on to the azimuth beambook characteristics. The UEs may point the antenna beam at all directions such that $\phi_{\text{UE}} \in [0, 360[\,°$. Therefore, there are either 30 pencil or 15 sector beam azimuth angles. Last, the BSs azimuth range is reduced to 270° due to building obstruction. Thus, there are 23 and 12 distinct BS beam azimuth angles ϕ_{BS}, respectively. Overall, this work considers three combinations of UE and BS antenna beam types and beambooks introduced above. Consequently, the number of beam pairs, and thus distinct directional CIRs, differs as summarized in Tab. II. When using *pencil beams* on both sides there are $(23 \cdot 8) \cdot (30 \cdot 8) = 44{,}160$ beam pairs, whereas just 2,880 with *sector beams*. In the third case, the BS uses pencil beams and the UE uses sector beams such that there are 11,040 entries in the *mixed beams* dataset.

B. Modeling of User Device Mobility Types

This work first investigates the performance of stationary beam training schemes, to be discussed in Sec. IV-C, before assessing the impact of post-beam training mobility (without compensation by beam tracking and switching) as follows: Here we consider *(i)* movement from the position of initial access to every possible position within the torus spanned by inner and outer radii $]r - 1\,\text{m}, r]$ with r being an integer in the range from 1 m to 9 m. Overall, 10 distributions with the

number of entries ranging from 110.000 (initial position) up to tens of million entries ($r = 9\,\mathrm{m}$) will be evaluated. Another important aspect is *(ii)* device rotation [7] by all angles up to 180° in steps of 12° for the pencil beams dataset or up to 168° in 24° steps when using sector beams on the UE side. The evaluation of the above mobility aspects considers up to 30 distributions over $4 \cdot 110.000$ initial user positions, where factor four comes from the leveraged UE side starting beam orientations for beam training, i.e., 0°, 96°, 192°, and 264°.

Last, we consider mobile beam training (like in Sec. III) at four velocities: 15 km/h, 25 km/h, 35 km/h, and 45 km/h. They represent typical urban traffic flows. Moreover, four trajectories for vehicles entering the crossing from different sides are considered as depicted in Fig. 6. We consider numerous individual routes per trajectory, e.g., there are 26 UE y-axis positions spanning a 5 m section across the eastward lanes. Moreover, the point in time at which the UE begins the beam training differs such that there are up to 120 different initial x-axis positions spaced in 1 m intervals. Overall, our evaluations consider up to 12,480 trajectories per velocity level with the initial UE side azimuth angle for beam training being fairly distributed among four approximately 90°-spaced directions.

C. Beam Training Algorithms

The exhaustive search algorithm is a well-known beam training approach which provides stationary users with the optimal beam pair, however, at the cost of the maximum delay. Like in an hierarchical search, it may also be used with sector beams instead of pencil beams to reduce the delay at the cost of reduced cell size for initial access [9]. For the sake of a representative evaluation of arbitrary beam training algorithms, we introduce a novel *quality of service (QoS)-aware beam search* algorithm that, in a greedy fashion, proactively terminates the exhaustive search once a predetermined QoS requirement Ψ_{th} is surpassed, as shown by the state diagram in Fig. 8. The threshold shall be intelligently determined based on predicted application layer requirements, UE mobility and radio condition parameters.

In this work, Ψ_{th} is defined in terms of RSS with the idea being that search time is reduced when aiming for reduced link quality. We note that this is partially motivated by the FastND algorithm [10] which terminates as soon as a control signal can be decoded. Here we use $\Psi_{\mathrm{th}} = -83.5\,\mathrm{dBm}$ for decodability, whereas exhaustive search is realized by setting Ψ_{th} to infinity. Moreover, we consider the arbitrary QoS thresholds of −70 dBm, −60 dBm, −50 dBm, and −40 dBm. We therefore use this greedy beam training algorithm with six thresholds and in combination with different BS-UE beam combinations to emulate a wide range of potential beam training algorithms.

D. Performance Metrics

Our evaluation in Sec. V incorporates the introduced dataset and the extensive mobility considerations using the parametrizable beam search scheme along with different beam types, cf. Secs. IV-A to IV-C. With ψ_{th} here being defined in terms of RSS, this work considers achieved RSS distributions along the entire evaluation area as well as the degradation thereof due to mobility. Similarly, we investigate the both coverage and mobility impacted IAF rate and the post-beam training mobility based RLFs rate. We also study the beam training delay which considers a rate of 64 beam pair measurements every 5 ms, like in Sec. III. The resulting delay, at the cost of increased BS signaling and energy consumption, is four times lower than with the 5G default 20 ms SS burst periodicity [5].

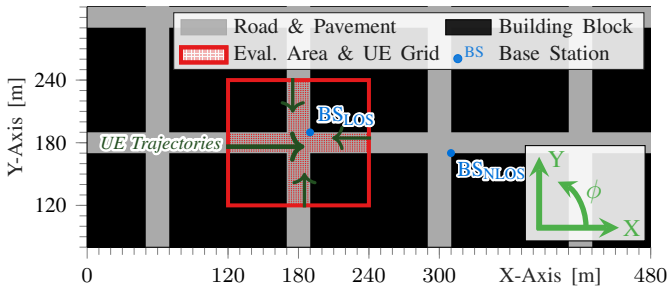

Fig. 6. mmWave BSs serve mobile UEs in metropolitan hotspot area. Ray-tracing based directional channel data for 110,000 positions is leveraged.

TABLE II. USED DATASETS CHARACTERIZED BY UE/BS BEAM TYPES.

Characterization of Datasets		*pencil*	*sector*	*mixed*
BS beam codebook	# az. angles ϕ (270° horizontal range)	23	12	23
	# el. angles θ (down to 90° downtilt)	8	4	8
UE beam codebook	# az. angles ϕ (360° horizontal range)	30	15	15
	# el. angles θ (up to 90° uptilt)	8	4	4
# beam pairs per dataset		44,160	2,880	11,040

– Pencil beams, cf. Fig. 7a. – Sector beams, cf. Fig. 7b.

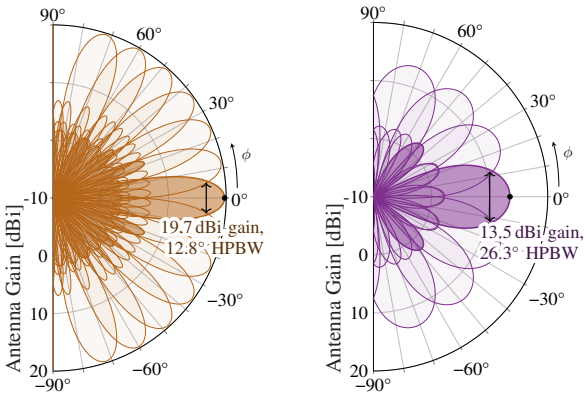

(a) Pencil beam codebook in uniform steps of 12°.

(b) Sector beam codebook in uniform steps of 24°.

Fig. 7. Azimuth plane beam patterns with gain and HPBW information.

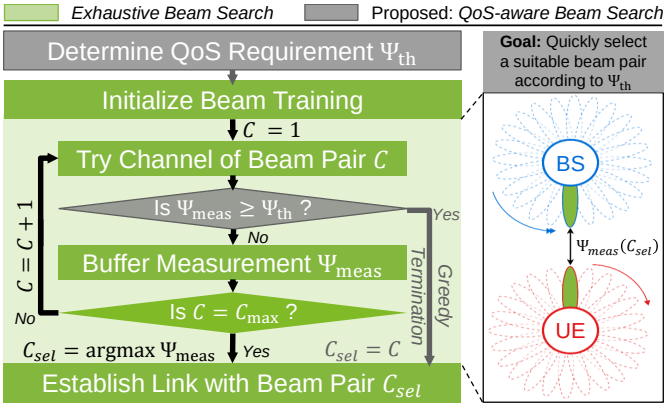

Fig. 8. Exhaustive search scheme and adaptions made for QoS-aware beam training selecting beam pair C_{sel}. In this work, Ψ is the RSS metric.

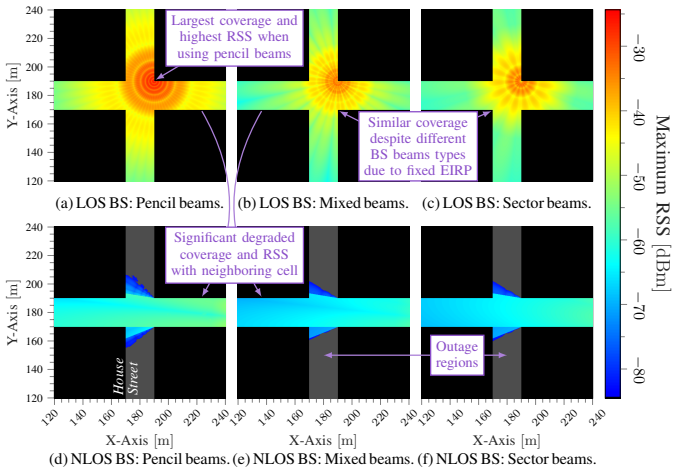

Fig. 9. Link strength of optimal beam pair depicted for every UE position.

V. Evaluation

This section is divided into three parts. First, Sec. V-A dives into the baseline performance consideration of a stationary UE. We then study the implications of user movement and device rotation after the beam training in Sec. V-B, neglecting beam tracking and switching-based compensation. Last, we evaluate the performance of mobile beam training in Sec. V-C.

A. Performance Benchmark: Stationary User

Using exhaustive search with different beam types, different RSSs are attained in the considered scenario, as shown in Fig. 9. The trade-off regarding the initial access cell size can be observed as pencil beams provide the street canyons with increased peak RSS compared to using other beam combinations. Moreover, the outage zones for the NLOS BS are smaller. This can also be seen in Fig. 10a in which the RSS distributions are depicted together with the IAF rate. There it can be observed that the use of mixed beams, i.e., pencil beam on BS side and sector beam on UE side, degrades the lower and upper tails of the RSS distributions compared to exclusively using sector beams, although the mean and median values are slightly increased. Considering the incurred beam training delay differences depicted in Fig. 10b, mixed beams are not preferable over sector beams. As such, we mainly compare pencil and sector beams based beam training. Moreover, we will focus our evaluation on the availability of a nearby LOS BS to avoid negative effects from the shadowing in the north and south street canyons, as the urban buildings effectively act as cell boundaries leading to failed beam training at up to 40.7 % of the evaluation area.

Moving on to using the proposed QoS-aware beam search algorithm which corresponds to exhaustive search if ψ_{th} demands infinite signal strength. The performance for lower RSS targets down to the decoding threshold is depicted in Fig. 11. Focusing on the beamforming performance when using pencil beams, cf. Fig. 11a, we find that the achieved RSS gets worse with reduced QoS threshold ψ_{th}, however, the beam training delay gets better. For the lowest threshold, the 0.23 s delay of a sector beam-based search is reached in 99.8 % of all cases, thus, we confirm that our proposed scheme is indeed able to tune the delay-RSS trade-off according to a single parameter. We note that the selected beam pair will still be refined over time after successful initial access in the scope of regular beam tracking and switching procedures. Considering the performance of $\psi_{\text{th}} = -70\,\text{dBm}$, we find that a link with a RSS gap of 13.5 dB to the decoding threshold can be attained at negligible additional delay. More robust links, however, come at the cost of longer searches such that increases of ψ_{th} do come with an increased delay penalty, e.g., for the threshold of −60 dBm just 60.7 % of pencil beam-based searches meet the delay of a sector beam-based exhaustive search. Additionally, one can observe with increasing ψ_{th} that more often the maximum delay is incurred as the network cannot serve sufficiently strong signals at these positions. Further considering the limited number of modulation and coding schemes (MCSs) in practice, the upper bound of ψ_{th} should naturally be chosen such that the highest MCS can just be used to reduce unnecessary beam training delay. The results for the use of our proposed greedy beam search using sector beams in Fig. 11b confirm this as the reduced available RSS from using less-directive beams makes the choice of high threshold above −60 dB infeasible as a significant reduction of beam training delay affects less than half of the UE grid. Last, we note that the beam training was successful at all positions.

B. Robustness to Mobility after Beam Training

As $\psi_{\text{th}} = -60\,\text{dBm}$ just turned out to be a good trade-off regarding incurred delay and achieved RSS, we will compare the impact of post-beam training mobility (cf. Sec. IV-B) for this algorithm setting of QoS-aware search to the exhaustive search: After first considering changed user positions in Sec. V-B1, we then assess the impact of UE rotation in Sec. V-B2.

1) UE Movement in Crossing Area: Fig. 12 puts forth the impact on the radio link acquired after beam training by moving from the original UE position by up to 9 m. In Fig. 12a an exhaustive pencil beam search was conducted. With increased movement the RSS distributions degrade and occasional link failures occur. After 8 m to 9 m, the median RSS drops by 15.7 dB but remains well above the decoding threshold such that high throughputs remain feasible. However,

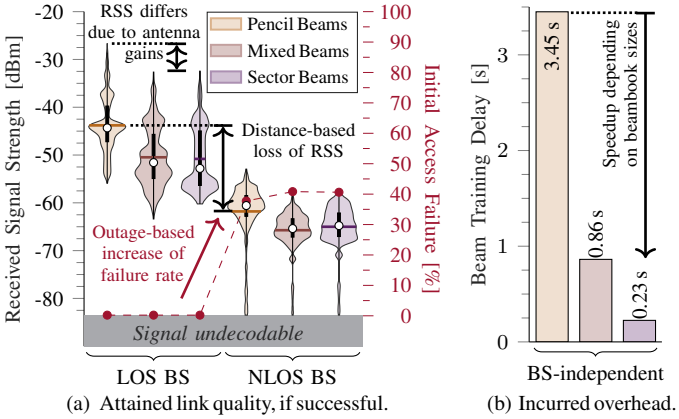

Fig. 10. Performance benchmark under stationary conditions: Exhaustive beam search-based beam training for different BS-UE beam combinations.

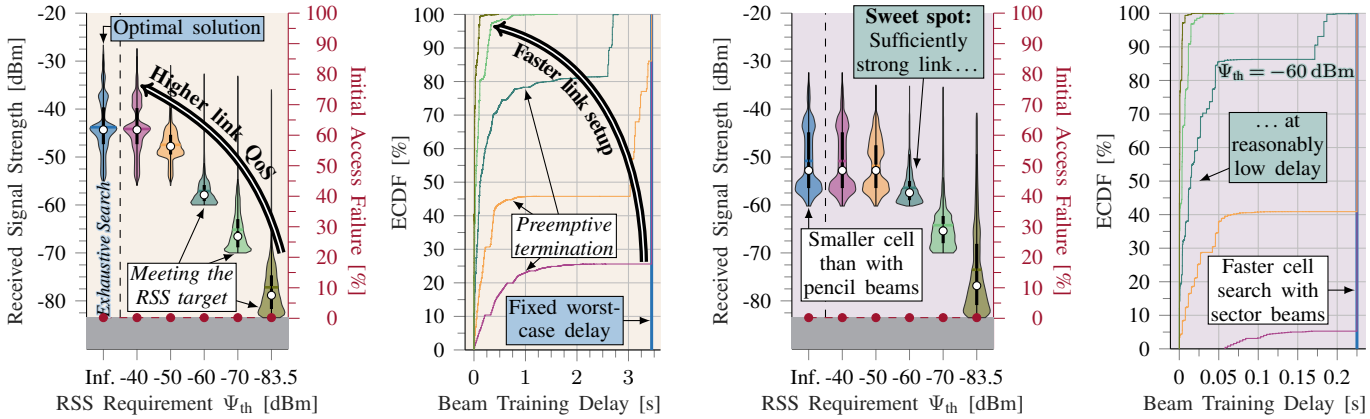

(a) Beam training with pencil beams.

(b) Beam training with sector beams.

Fig. 11. Performance of greedy beam search under stationary conditions for UEs connecting to the nearby LOS BS using *(a)* pencil or *(b)* sector beams. Comparison for termination at different QoS thresholds in terms of target RSS level: *(left)* attained RSS with IAF rate, and *(right)* incurred delay.

the link is lost in 17.8 % of all cases. When using the proposed QoS-aware pencil beam search, cf. Fig. 12b, the likelihood of a RLF grows as it happens in 33.7 % of all user movements of 8 m to 9 m. The median RSS is an additional 9.6 dB lower than for the exhaustive pencil beam search, thus illustrating that the greedy beam training, which typically terminates quickly by selecting a degraded link, needs to be more actively compensated by beam management after the initial access.

Moving on to the performance when using sector beams. Comparing Fig. 12c to the previously discussed Fig. 12a, increased robustness against mobility can be observed with reduced loss in RSS and reduced likelihood for link failures after 8 m to 9 m UE movement. We make similar observations for our proposed greedy algorithm, cf. Figs. 12b and 12d, but note that the use of sector beams reduces the impact of user mobility more drastically. This underlines that mmWave link maintenance for sector beams is less pressing than when using pencil beams and particularly, that when using sector beams there is just a negligible impact by the beam training algorithm, as long as only a reasonably greedy parametrization is considered.

2) Horizontal Rotation of UE: Let us now consider the impact of uncompensated user rotation on the acquired link with dependency on the used beam training algorithm and beam types, as shown in Fig. 13. Considering a prior pencil beam search-based initial access, cf. Fig. 13a, we find that fine rotations by 12° or 24° symmetrically degrade the median RSS by 12.2 dB to 15.2 dB, respectively. However, the RLF rate remains low until rotating by 72°. We note that this would mean in practical systems that rotations within the antenna array's field of view do not necessarily lead to link failures, although the median RSS is now degraded by more than 22.4 dB which would be a problem if the user is near the cell boundary. Rotations by more than 72° lead to an interrupted connection in more than 90 % of all cases, i.e., compensation for such large device rotations is essential in any case. When using sector beams, we observe very similar behavior in Fig. 13c, thus illustrating that user rotation, contrary to simple movement, has a severe impact regardless of the antenna beam types being used. Considering that device rotations are much more easily conducted than a movement by, for example, 9 m as studied before, this shows that beam tracking and switching in future 6G networks need to be capable of compensating for the severe impact of user rotation. When this problem is solved, link maintenance for simple user motion is most likely already handled by default.

Moving on, we now also briefly consider the impact of the choice of beam training algorithm on the impact of user rotation. Fig. 13b now lacks symmetry compared to Fig. 13a which is due to the greedy termination of the beam training before the optimal beam pair is identified. As such, the rotation in the one direction may lead to a better link quality as this orientation has not yet been measured before and might be better than the selected beam orientation, whereas the other direction has already been tested and exhibited a weaker RSS than the chosen beam pair. We observe a similar impact of the horizontal user device rotation using sector beams, cf. Fig. 13d. Here, we identify that greedy beam training softens the likelihood of RLFs due to rotation, however, the remaining RSS level becomes unpredictable. If a very low ψ_{th} is used, e.g., −83 dBm, which is not depicted in this work for brevity, this conclusion needs to be altered: Whereas the RSS remains unpredictable if the link is kept, the RLF rate is drastically increased to above 50 % even for rotations as little as 24°. This demonstrates that suboptimal beam alignments due to reduced beam training delay increase susceptibility to mobility-induced mmWave link failures.

C. Impact of User Mobility during Beam Training

Last, we consider how user mobility during the beam training impacts the initial access success rate and attained link quality. As detailed in Sec. IV-B, we consider straight trajectories through the crossing at different velocities up to 45 km/h. When using pencil beams with different beam training algorithms, we find the following performance in Fig. 14a. At 15 km/h, exhaustive search begins to select misaligned beams thus establishing degraded links. Although this affects less than 50 % of all trajectories (median loss 0 dB), the mean loss in RSS is already 8.9 dB. Moreover, in 31.8 % the initial access fails which is undesirable and marks a significant contrast to its optimal performance under stationary

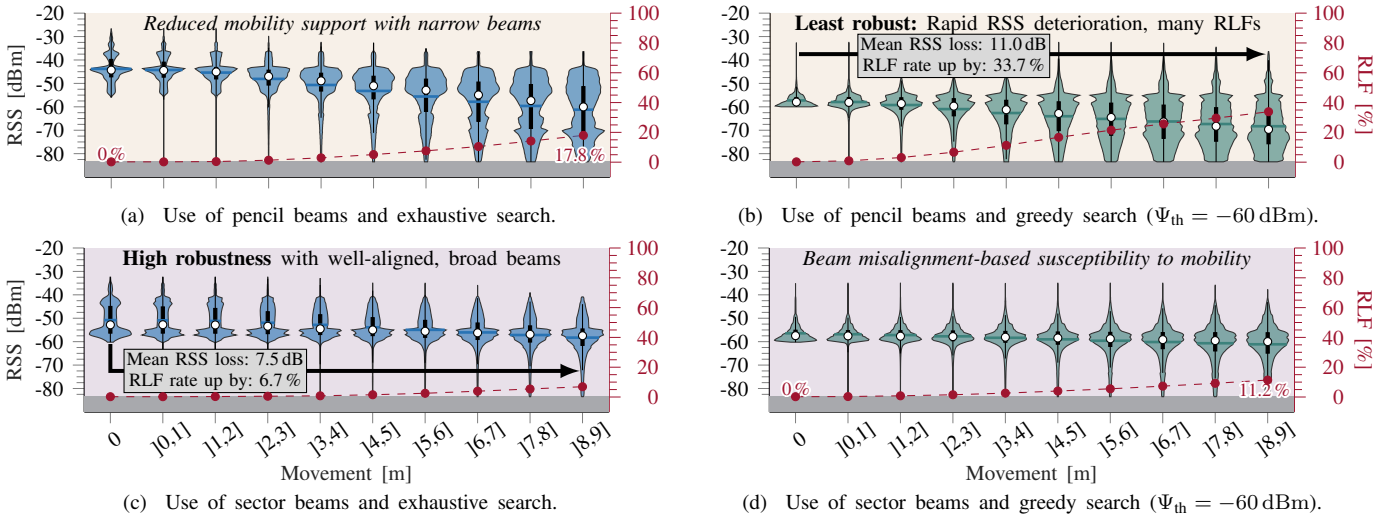

(a) Use of pencil beams and exhaustive search.

(b) Use of pencil beams and greedy search ($\Psi_{\text{th}} = -60\,\text{dBm}$).

(c) Use of sector beams and exhaustive search.

(d) Use of sector beams and greedy search ($\Psi_{\text{th}} = -60\,\text{dBm}$).

Fig. 12. Assessment of the channel state according to the distance moved by the user, considering initial access under stationary LOS conditions. The impact on received power (RSS) and link failure (RLF) metrics is illustrated in *(a)-(d)* for different BS-UE beam combinations and bean training schemes.

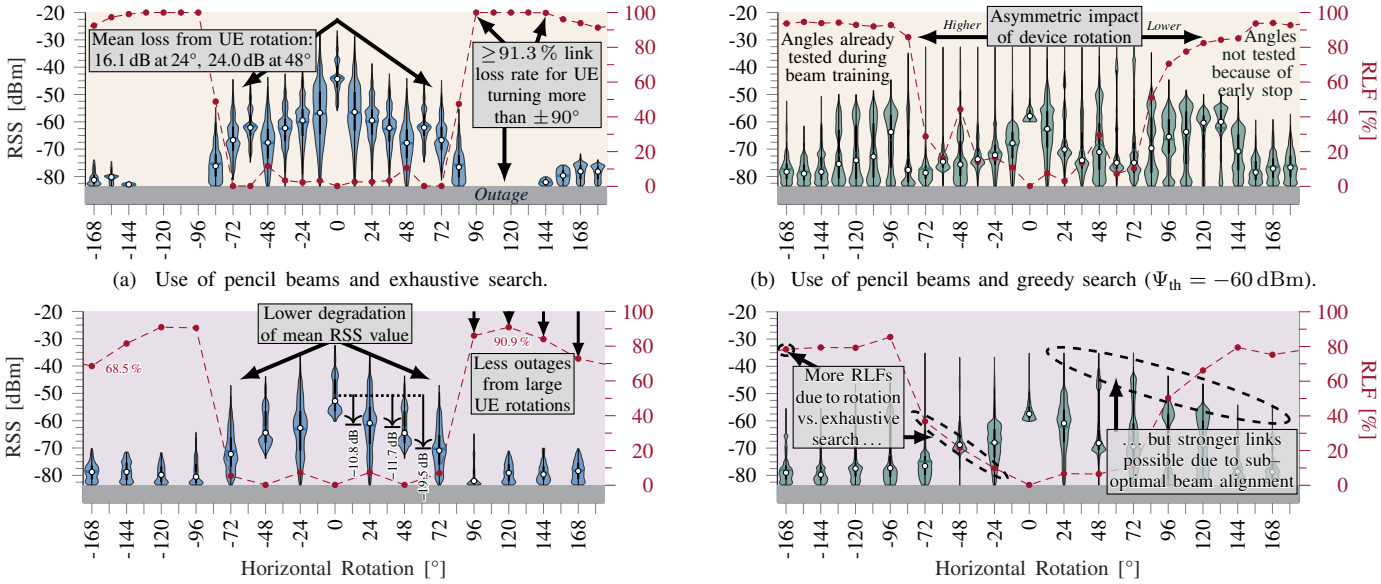

(a) Use of pencil beams and exhaustive search.

(b) Use of pencil beams and greedy search ($\Psi_{\text{th}} = -60\,\text{dBm}$).

(c) Use of sector beams and exhaustive search.

(d) Use of sector beams and greedy search ($\Psi_{\text{th}} = -60\,\text{dBm}$).

Fig. 13. Impact of sudden horizontal UE rotations right after initial access under LOS conditions. Channel states depicted in *(a)-(d)* depend on the used BS-UE beam combination and the beam training algorithm. As such, target reaction times for link maintenance procedures need to be defined accordingly.

conditions, cf. Sec. V-A. Increasing the user velocity, mean and median loss increase beyond 20 dB, and IAFs are incurred in 52.6 % (25 km/h), 70.3 % (35 km/h), and 81.4 % (45 km/h) of all cases, respectively. This makes an exhaustive search with highly directional pencil beams already infeasible for mobile initial access at typical urban velocities.

Regarding Fig. 14a, and including our observations from Secs. V-A and V-B, we now compare the proposed QoS-aware beam training algorithm, cf. state machine in Fig. 8, to exhaustive search for selected predetermined link requirements:

- *High QoS target* ($\psi_{\text{th}} = -40\,\text{dBm}$, i.e., max. throughput): Under stationary conditions, cf. Fig. 11a, this choice reduces the search time drastically in about 25 % of all cases with negligible impact on the data rate. Here, scaling with user velocity, we additionally observe reduced mean and interquartile range losses as well as drastically fewer IAFs than exhaustive search, thus demonstrating superior support for mobile beam training owing to a minor change.
- *Low QoS target* ($\psi_{\text{th}} = -83.5\,\text{dBm}$, i.e., decodable signaling): Using the lowest possible target link strength reliably reduces the beam training delay down to a fraction of a second for stationary users, as previously observed in Fig. 11a. Moreover, the attained link is much more likely to be lost due to post-beam training mobility, particularly device rotation, cf. Sec. V-B2. However, this comes at great losses which may also be observed for mobile beam training, however, at high velocities such as at 45 km/h this is nonetheless preferable over using exhaustive search: Whereas mean and median delays are higher and the distribution is centered around a fixed loss greater than 20 dB, the greedy scheme's loss distribution tail is curbed such that very high losses are observed less often and, importantly, no single IAF com-

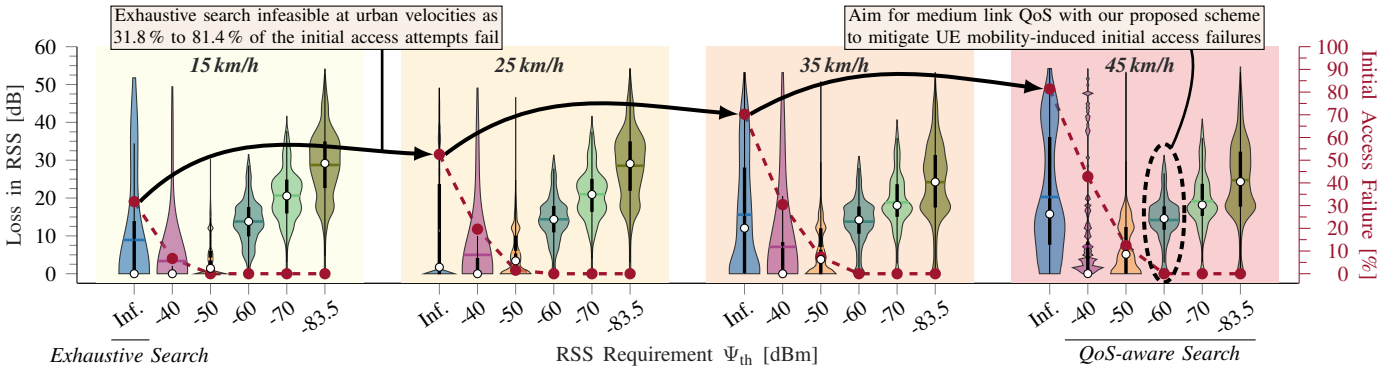

(a) Pencil beams-based training performance deteriorates with UE mobility. The proposed scheme avoids severe initial access failures.

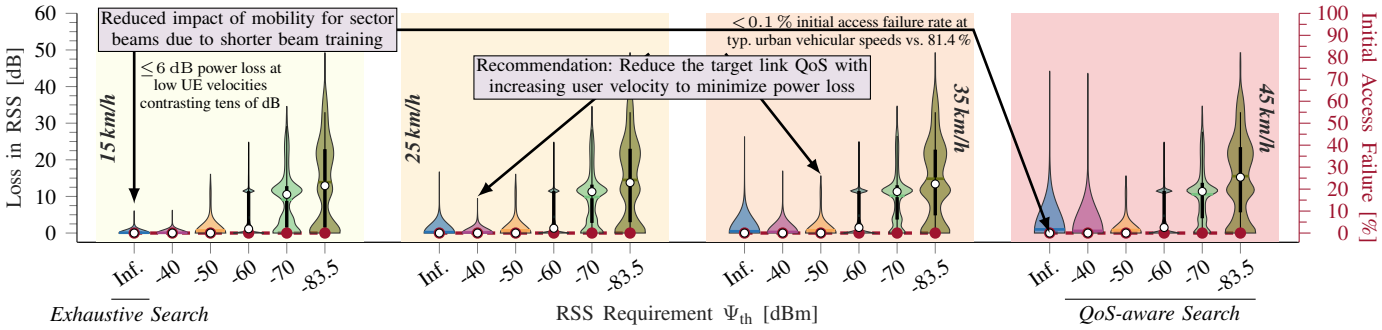

(b) Whereas mobile cell search with sector beams does not suffer from access failures, incurred power losses can be minimized with our approach.

Fig. 14. Analysis of initial access for mobile users with different beam types and training schemes. Loss in RSS is determined for the position at which the beam training is successfully completed, comparing the selected with the optimal beam combination. The second y-axis tracks the IAF rate.

pared to more than 81.3 %. For the considered velocities, the loss distribution seems mostly invariant to the user mobility, but the mean loss reduces for increasing velocities. This underlines that deliberate greedy beam training is desirable for highly-mobile UEs which marks a contrast to the popular approach aiming for the optimal beam pair.

- *Medium QoS target* ($\psi_{\text{th}} = -60\,\text{dBm}$): Let us now consider our QoS-aware beam search that is parametrized such that a balanced performance between beam training delay and beam misalignment-based power loss is attained, cf. evaluation in Sec. V-A. For increasingly mobile users, we observe the following desirable characteristics combining the points highlighted for the previously discussed two unbalanced parametrizations: At 45 km/h, a mean loss in RSS of just 14.2 dB is observed with IAFs being mitigated. This marks improvements by 6.1 dB and 81.4 percentage points over exhaustive search, respectively. Compared to using a higher QoS, the chances for successful mobile initial access increase due to the reduced beam training delay, however, at the cost of some increased loss affecting the throughput. This indicates that the sweet spot for Ψ_{th} could be right between −50 dBm to −60 dBm. If a lower QoS were used, all initial access attempts would remain successful due to even faster beam training, however, higher losses would make the attained links less robust to the ongoing mobility until beam tracking and switching mechanisms have set in.

Extending the discussion of the previous paragraph, we now study the delay of mmWave beam training for mobile users, as depicted in Fig. 15. At first glance, we observe similar latency distributions as for the stationary case, cf. Fig. 11a. However, we find that our proposed QoS-aware beam search algorithm tends to terminate even quicker for mobile UEs. This is observed for well-parametrized Ψ_{th} values, i.e., when aiming for a RSS far above the decoding threshold but not necessarily for the optimal beam combination or beyond what is needed to support the maximum MCS. Studying the distributions more closely, we do not see any latency gains where the training is already sped up compared to the exhaustive search, but where UEs needed a long beam training beforehand. This indicates that UEs in low-connectivity regions, i.e., with high channel sparsity, experience a higher connectivity due to mobility such that the beam training delay may be reduced. We note that this is another benefit of the preemptive termination of the proposed scheme adding to the major benefits of reducing initial access failure rate and power loss during mobility.

We move on to mobile beam training using sector beams, as shown in Fig. 14b. Compared to when using pencil beams, mobile UEs employing exhaustive search and greedy beam training schemes, e.g., aiming for $\psi_{\text{th}} = -40\,\text{dBm}$, do not suffer from strong mobility-induced losses. More importantly, the risk of an IAF is mitigated. This underlines our previous results from Sec. V-A, that reduced beam training delay through using fewer but broader beams increases support for mobile mmWave initial access at the cost of a smaller cell size due to lower antenna gain. Nonetheless, it may be observed that even here reasonably "greedy" schemes become increasingly suitable at very high velocities because the loss of signal strength may be minimized while also reducing the beam training-based delay for the initial access. In fact, the performance then exceeds the "optimal" approach, noting that

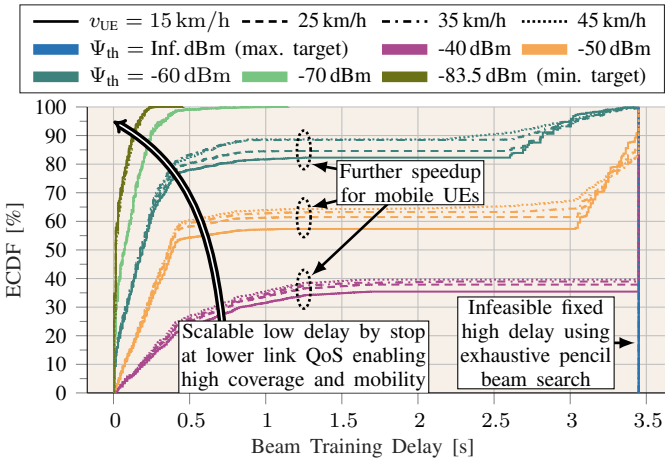

Fig. 15. Delays for mobile beam training using pencil beams on either side. The QoS-aware beam search scheme experiences a speedup that grows with the UE velocity, thus adding to the previously identified benefits.

these traditional classifications of "greedy" and "optimal" only pertain to stationary conditions. Referring back to Fig. 3, our findings underline the initially suggested hypothesis that a beam training scheme's mobility support is indeed a consideration that extends the typical three-way design trade-off. As such, future 6G mmWave nodes have to employ protocols designed in consideration of all four aspects.

Noting that we assumed the highest possible 5G signaling rate of 64 SS blocks per 5 ms instead of the 20 ms default value, cf. Sec. IV-D, we must also highlight that this reduces the impact of mobility. Energy-efficient deployments may even extend the burst periodicity to 160 ms [5], effectively scaling the impact of UE velocity by a factor greater than 30. To address the resulting high failure rate of mobile beam training, such algorithms should terminate preemptively when a sufficiently qualitative beam pair is detected to avoid detrimental staleness-induced initial access failures. Because of this, beam misalignments will likely initially degrade the link strength, but can be mitigated by beam refinement procedures that maintain the connection during ongoing user mobility.

VI. Conclusions

In this paper, we investigated the differences between stationary and mobile mmWave beam training procedures. We observed in both the laboratory experiment and the simulation study that exhaustive search incurs power losses in the tens of decibels depending on velocity, contrasting its optimal performance in stationary conditions. Even worse, our urban ray-tracing study further showed that more than 81.4 % of all initial access attempts failed at 45 km/h owing to data staleness. Hence, the fixed long delay for all pencil beam combinations makes it an infeasible choice for urban deployments. At the undesirable cost of reduced cell size, hierarchical approaches initially using sector beams can be employed to reduce the delay, thus postponing the above behavior to higher velocities. We further found the initial access with broad beams prior to pencil beam refinement to also increase robustness against ongoing post-beam training mobility, thereby relaxing the time constraints for beam tracking and switching mechanisms. Nonetheless, sudden UE rotations would need to be addressed with utmost priority.

Addressing the low mobility support by exhaustive search, we then proposed the QoS-aware beam search that terminates once the predetermined link quality threshold is met. Configured to the sweet spot, here −60 dBm receive power, beam training delays are limited to below 0.5 s in 75 % of all runs, but enable high data rates despite of using pencil beams. For mobile users, this configuration also drastically reduces losses and, in particular, mitigates initial access failures at 45 km/h entirely. Thus, we demonstrated an improved beam training scheme that increases the mobile mmWave connectivity experience by discouraging a long procedure that may introduce staleness. As such, we conclude that the design goal for 6G beam training changes from establishing the best possible link to terminating once a sufficiently suitable beam pair is found, e.g., with 20 dB link margin. Our investigation also showed that this necessitates more rapid link maintenance immediately after the initial access to compensate for the ongoing user mobility, but more of such activity is not unexpected for 6G due to the transition from stationary to mobile use cases.

References

[1] M. Giordani, M. Mezzavilla, and M. Zorzi, "Initial access in 5G mmWave cellular networks," *IEEE Commun. Mag.*, vol. 54, no. 11, 2016.

[2] K. Heimann, J. Tiemann, D. Yolchyan, and C. Wietfeld, "Experimental 5G mmWave beam tracking testbed for evaluation of vehicular communications," in *Proc. IEEE 5GWF*, 2019.

[3] N. Michelusi and M. Hussain, "Optimal beam-sweeping and communication in mobile millimeter-wave networks," in *Proc. IEEE ICC*, 2018.

[4] W.-T. Shih *et al.*, "Fast antenna and beam switching method for mmWave handsets with hand blockage," *IEEE Trans. Wirel. Commun.*, vol. 20, no. 12, 2021.

[5] A. Ichkov, S. Häger, P. Mähönen, and L. Simić, "Comparative evaluation of millimeter-wave beamsteering algorithms using outdoor phased antenna array measurements," in *Proc. IEEE SECON*, 2022.

[6] J. Palacios, D. De Donno, and J. Widmer, "Tracking mm-Wave channel dynamics: Fast beam training strategies under mobility," in *Proc. IEEE INFOCOM*, 2017.

[7] Y. Heng *et al.*, "Six key challenges for beam management in 5.5G and 6G systems," *IEEE Commun. Mag.*, vol. 59, no. 7, 2021.

[8] 3GPP Technical Report (TR) 38.300 v18.0.0, "TSG RAN; NR; NR and NG-RAN overall description; stage 2 (release 17)," 2024.

[9] L. Wei, Q. Li, and G. Wu, "Exhaustive, iterative and hybrid initial access techniques in mmWave communications," in *Proc. IEEE WCNC*, 2017.

[10] A. Zhou *et al.*, "FastND: Accelerating directional neighbor discovery for 60-GHz millimeter-wave wireless networks," *IEEE/ACM Trans. Netw.*, vol. 26, no. 5, 2018.

[11] H. Hassanieh *et al.*, "Fast millimeter wave beam alignment," in *Proc. ACM SIGCOMM*, 2018.

[12] S. Sur *et al.*, "Towards scalable and ubiquitous millimeter-wave wireless networks," in *Proc. ACM MobiCom*, 2018.

[13] S. Wang, J. Huang, and X. Zhang, "Demystifying millimeter-wave V2X: Towards robust and efficient directional connectivity under high mobility," in *Proc. ACM MobiCom*, 2020.

[14] A. Ichkov *et al.*, "Millimeter-wave beam misalignment effects of small- and large-scale user mobility based on urban measurements," in *Proc. ACM mmNets*, 2021.

[15] M. Cheng *et al.*, "A fast beam searching scheme in mmWave communications for high-speed trains," in *Proc. IEEE ICC*, 2019.

[16] S. H. Lim *et al.*, "Efficient beam training and sparse channel estimation for millimeter wave communications under mobility," *IEEE Trans. Wirel. Commun.*, vol. 68, no. 10, 2020.

[17] K. Heimann, S. Häger, and C. Wietfeld, "Demo abstract: Experimental 6G research platform for digital twin-enabled beam management," in *Proc. ACM MobiWac*, 2023, video: https://tiny.cc/HeliosDemonstrator.

[18] S. Häger, K. Heimann, S. Böcker, and C. Wietfeld, "Holistic enlightening of blackspots with passive tailorable reflecting surfaces for efficient urban mmWave networks," *IEEE Access*, vol. 11, 2023.

[19] S. Häger, N. Gratza, and C. Wietfeld, "Characterization of 5G mmWave high-accuracy positioning services for urban road traffic," in *Proc. IEEE VTC-Spring*, 2023.